VOLUME 121, NUMBER 15
APRIL 21, 1999

JOURNAL OF THE AMERICAN CHEMICAL SOCIETY

Interactions of TMPyP4 and TMPyP2 with Quadruplex DNA. Structural Basis for the Differential Effects on Telomerase Inhibition

Frank Xiaoguang Han, Richard T. Wheelhouse, and Laurence H. Hurley*

Contribution from the Drug Dynamics Institute, College of Pharmacy, The University of Texas at Austin, Austin, Texas 78712-1074

Received December 1, 1998

Abstract: The cationic porphyrins TMPyP4 and TMPyP2 possess similar structures but have strikingly different potencies for telomerase inhibition. To rationalize this difference, the interactions of TMPyP4 and TMPyP2 with an antiparallel quadruplex DNA were investigated. A single-stranded DNA oligonucleotide (G4A) containing four human telomere repeats of GGGTTA has been designed to form an intramolecular quadruplex DNA and was confirmed to form such a structure under 100 mM KCl by a DNA ligase assay, DMS footprinting, and CD spectrum analysis. By carrying out UV spectroscopic studies of the thermal melting profiles of G4A−porphyrin complexes, we provide evidence that TMPyP4 and TMPyP2 both stabilize quadruplex DNA to about the same extent. A photocleavage assay was used to determine the precise location for TMPyP4 and TMPyP2 in their interactions with quadruplex DNA. The results show that TMPyP4 binds to the intramolecular quadruplex DNA by stacking externally to the guanine tetrad at the GT step, while TMPyP2 binds predominantly to the same G4 DNA structure via external binding to the TTA loop. We propose that the inability of TMPyP2 to bind to the G4A by stacking externally to the guanine tetrad accounts for the differential effects on telomerase inhibition by TMPyP4 and TMPyP2.

Introduction

Telomerase is active in over 90% of human tumor cell lines and is low or undetectable in normal somatic cells.[1−4] It has been proposed that telomerase activity is needed for tumor cell proliferation;[5,6] therefore, telomerase presents a potential selective target for the design of new antitumor drugs.[3] In the absence of an X-ray crystal structure of telomerase, however, the design of inhibitors that directly target telomerase has been difficult. One approach is the antisense strategy that targets the telomerase RNA component, which is essential for telomerase activity.[7] Another approach would be to target the G-quadruplex DNA that has been proposed to be associated with the telomerase reaction cycle.[8,9] In this regard, work from this laboratory has demonstrated that compounds that interact with G-quadruplex to stabilize this structure do inhibit telomerase.[10−12] The cationic porphyrin compound 5,10,15,20-tetra-(*N*-methyl-4-pyridyl)por-

* Address correspondence to this author.

(1) Shay, J. W.; Bacchetti, S. *Eur. J. Cancer* **1997**, *33*, 787−791.
(2) Shay, J. W.; Gazdar, A. F. *J. Clin. Pathol.* **1997**, *50*, 106−109.
(3) Holt, S. E.; Wright, W. E.; Shay, J. W. *Eur. J. Cancer* **1997**, *33*, 761−766.
(4) Kim, N. W.; Piatyszek, M. A.; Prowse, K. R.; Harley, C. B.; West, M. D.; Ho, P. L.; Coviello, G. M.; Wright, W. E.; Weinrich, S. L.; Shay, J. W. *Science* **1994**, *266*, 2011−2015.
(5) Greider, C. W. *Annu. Rev. Biochem.* **1996**, *65*, 337−365.
(6) Langford, L. A.; Piatyszek, M. A.; Xu, R.; Schold, S. C., Jr.; Wright, W. E.; Shay, J. W. *Hum. Pathol.* **1997**, *28*, 416−420.
(7) Hamilton, S. E.; Pitts, A. E.; Katipally, R. R.; Jia, X.; Rutter, J. P.; Davies, B. A.; Shay, J. W.; Wright, W. E.; Corey, D. R. *Biochemistry* **1997**, *36*, 11873−11880.
(8) Shippen-Lentz, D.; Blackburn, E. H. *Science* **1990**, *247*, 546−552.
(9) Zahler, A. M.; Williamson, J. R.; Cech, T. R.; Prescott, D. M. *Nature* **1991**, *350*, 718−720.
(10) Sun, D.; Thompson B.; Cathers, B. E.; Salazar, M.; Kerwin S. M.; Trent, J. O.; Jenkins, T. C.; Neidle, S.; Hurley, L. H. *J. Med. Chem.* **1997**, *40*, 2113−2116.

10.1021/ja984153m CCC: $18.00
Published on Web 04/03/1999

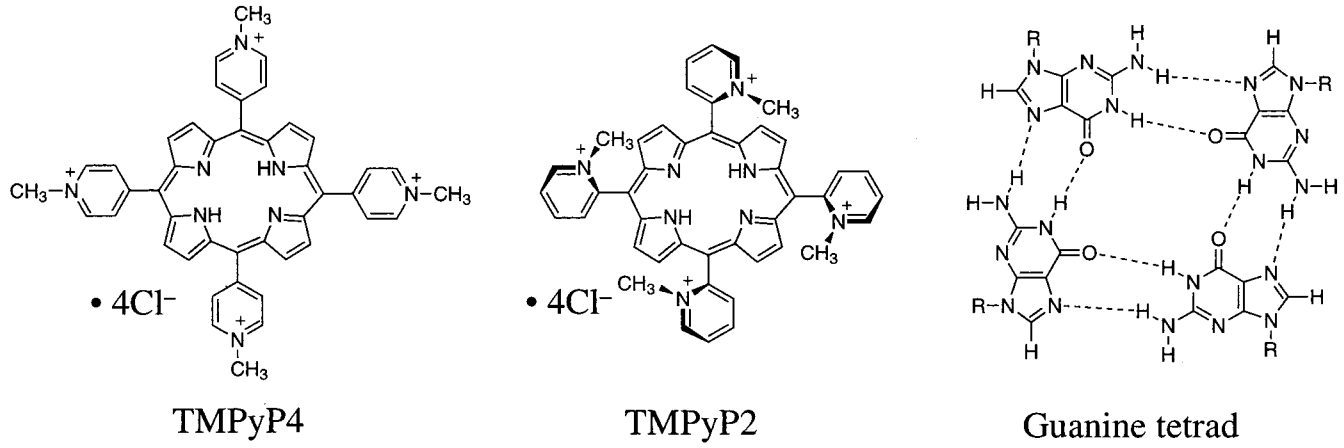

Figure 1. Structures of TMPyP4, TMPyP2, and the guanine tetrad.

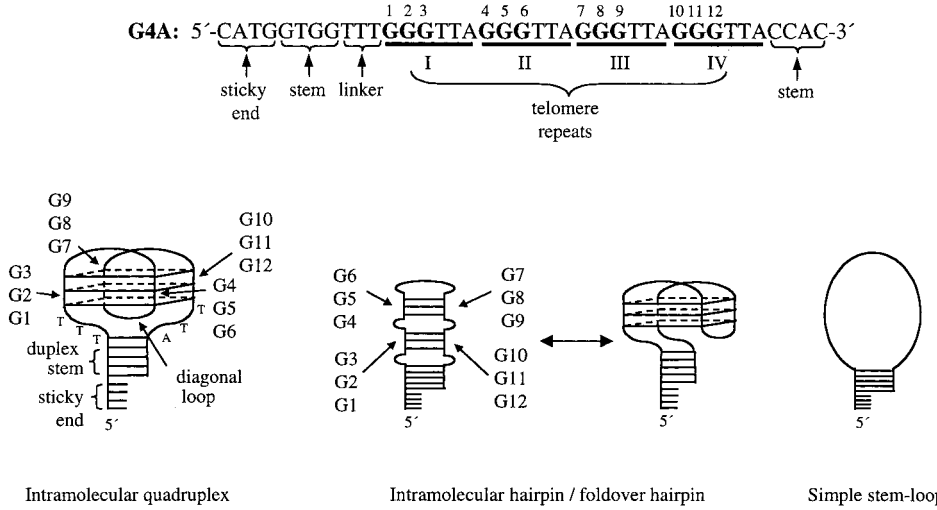

Figure 2. Sequence of G4A DNA and the three possible antiparallel secondary structures. The four GGGTTA telomeric repeats are numbered I, II, III, and IV, and the guanines in the four telomeric repeats are numbered 1 through 12. The three possible antiparallel secondary structures are the intramolecular quadruplex, the intramolecular hairpin, which can isomerase to a foldover hairpin, and the simple stem−loop.

phine (TMPyP4, structure shown in Figure 1) possesses the appropriate physical properties, including the molecular size, a planar chromophore, positive charges, and hydrophobicity, favorable for intercalating into or stacking with the guanine tetrads (Figure 1). In recent studies, TMPyP4 was shown to interact with quadruplex DNA[11,13] to produce telomerase inhibition in an in vitro assay using HeLa cell extract.[11] In contrast, the positional isomeric cationic porphyrin 5,10,15,20-tetra-(*N*-methyl-2-pyridyl)porphine (TMPyP2, structure shown in Figure 1) has an IC_{50} value that is more than 10-fold higher for telomerase inhibition (Sun and Hurley, unpublished results). The only difference between TMPyP4 and TMPyP2 is the position (ortho vs para) of the *N*-methyl group on the pyridyl ring relative to its connection to the porphine core. In an attempt to account for the structure−activity relationship of these two compounds with respect to telomerase inhibition, we have compared their interactions with an antiparallel guanine quadruplex DNA. By using CD and UV thermal melting studies in combination with a DNA photocleavage assay, we present evidence that TMPyP4 and TMPyP2 both interact with and stabilize quadruplex DNA to the same extent, but they do so by structurally distinct modes. TMPyP4 binds to the intramolecular quadruplex DNA formed by human telomere DNA repeats $(GGGTTA)_4$ by stacking externally with the guanine tetrad and exhibits strong selectivity for quadruplex DNA over duplex DNA. TMPyP2 does not bind to the intramolecular quadruplex DNA by direct stacking or by intercalating with the guanine tetrad. Instead, it interacts primarily with the quadruplex DNA by binding to the TTA loop, which is absent in the normal intramolecular quadruplex DNA structure. From this study, we propose that the different binding modes of TMPyP4 and TMPyP2 to quadruplex DNA may provide the structural basis for the differential telomerase inhibitory effects of these two compounds.

Materials and Methods

Synthesis of Oligonucleotide DNA. Oligonucleotide G4A (sequence shown in Figure 2) was synthesized using a PerSeptive Biosystems DNA synthesizer (model 8909) and purified by polyacrylamide gel electrophoresis. DNA concentration was determined spectrophotometrically at 260 nm.

Porphyrin Physiochemical Properties. The porphyrins did not contribute significantly to the absorbance at 260 nm. In addition, TMPyP2 and TMPyP4 did not aggregate under the conditions of our experiments and thus obeyed Beers Law. Because of the restricted rotation of the 3-methyl pyridyl rings, a statistical distribution of isomers

(11) Wheelhouse, R. T.; Sun, D.; Han, H.; Han, F. X.; Hurley, L. H. *J. Am. Chem. Soc.* **1998**, *120*, 3261−3262.
(12) Fedoroff, O. Yu.; Salazar, M.; Han, H.; Chemeris, V. V.; Kerwin, S. M.; Hurley. L. H. *Biochemistry* **1998**, *37*, 12367−12374.
(13) Arthanari, H.; Basu, S.; Kawano, T. L.; Bolton, P. H. *Nucleic Acids Res.* **1998**, *26*, 3724−3728.

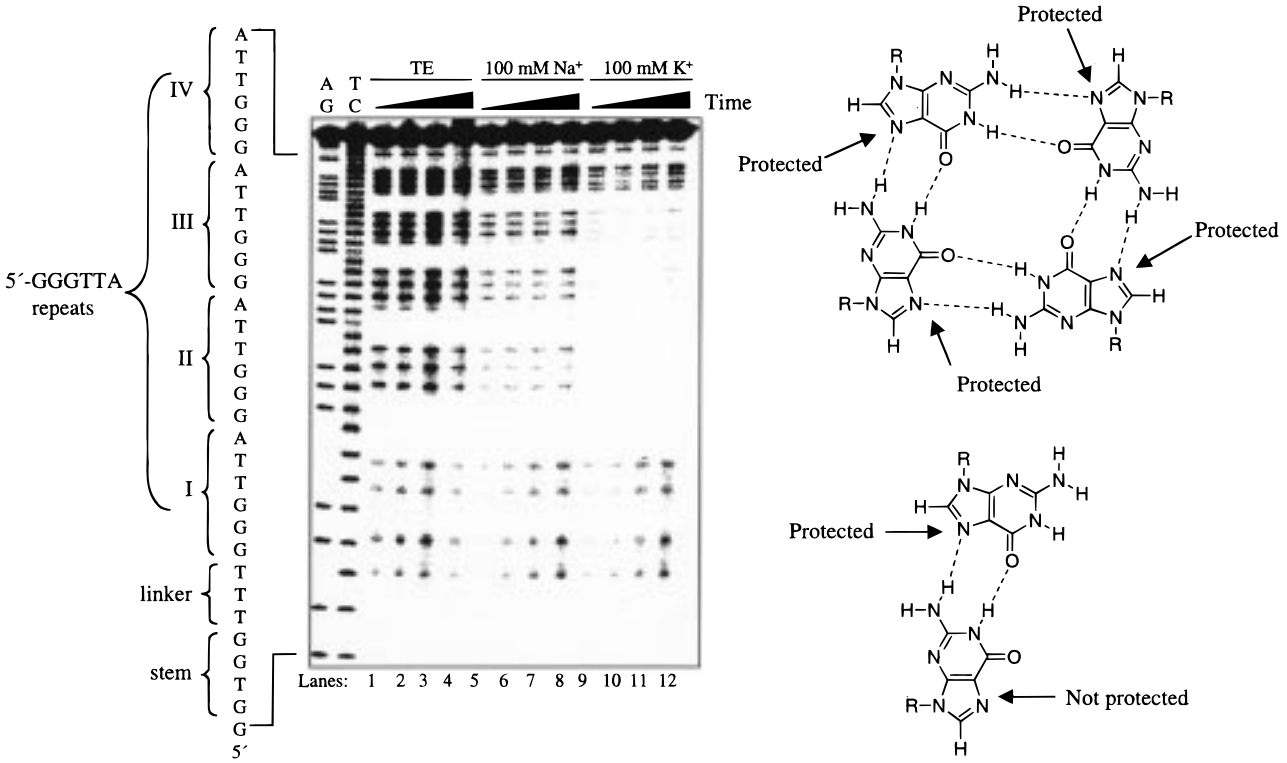

Figure 3. DMS footprinting assay of G4A in the control TE, Na^+, and K^+ buffers. Lanes AG and TC are the Maxam−Gilbert sequencing reactions. Lanes 1−4 are DMS footprinting of G4A DNA in the control buffer corresponding to reaction times of 1, 2, 5, and 10 min, respectively. Lanes 5−8 and lanes 9−12 are the same reactions performed in the Na^+ and K^+ buffers, respectively. In the guanine tetrad (top structure on the right), all of the guanines are protected from DMS modification at the N7 positions by forming hydrogen bonds. In the guanine−guanine hairpin (bottom structure on the right), only one N7 is protected. The partial sequence of G4A and its components is shown on the left side of the gel.

should be found in solution. Although we are consequently working with a mixture, we consider it doubtful that this will be a significant factor in interpretation of the results of the experiments described here.

Ligase Assay and *Exo*III Nuclease Digestion. For each ligation reaction, 10 μL of ^{32}P-labeled DNA (∼5 ng) was mixed with 10 μL of a 200 mM solution of either KCl or NaCl. The mixture was boiled for 10 min and then cooled to room temperature. Two microliters of a 10× concentration of ligase buffer (500 mM Tris-HCl, 100 mM $MgCl_2$, 100 mM DTT, 10 mM ATP, 500 μg/mL BSA, pH 7.8) and 1 μL of ligase (New England Biolabs) were then added. The reaction was incubated overnight at 16 °C and inactivated by heating to 70 °C for 20 min. Aliquots of each ligation reaction were further treated with 20 units of *Exo*III nuclease (from Gibco BRL) at 37 °C for 15, 30, and 60 min. The samples were then subjected to phenol extraction, ethanol precipitation, and 8% denaturing polyacrylamide gel electrophoresis.

Dimethyl Sulfate (DMS) Footprinting. For each reaction, 10 μL of ^{32}P-labeled DNA (20 000 cpm; ca. 5 ng) was mixed with 10 μL of a 200 mM solution of either KCl or NaCl, and this mixture was boiled for 10 min and then cooled to room temperature. Two microliters of 2% DMS was added for various times, as indicated in the caption to Figure 3. The reaction was stopped with 80 μL of DMS stop buffer (2 μL of 98% β-mercaptoethanol, 10 μL of 1 μg/μL calf thymus DNA, and 68 μL of distilled water). The DNA samples were then subjected to ethanol precipitation, piperidine treatment, and 16% polyacrylamide gel electrophoresis.

Circular Dichroism (CD) Spectroscopy. Five micromolar solutions of G4A were prepared in three different buffers: a TE buffer (4 mM Tris-HCl, 1 mM EDTA, pH 7.5), a Na^+ buffer (4 mM Tris-HCl, 1 mM EDTA, 100 mM NaCl, pH 7.5), and a K^+ buffer (4 mM Tris-HCl, 1 mM EDTA, 100 mM KCl, pH 7.5). These solutions were first heated to 95 °C for 5 min and then cooled to room temperature overnight. The CD spectra from wavelength 220 to 320 nm were recorded with a JASCO J-600 spectropolarimeter.

UV Thermal Melting Studies. Solutions of 0.75 μM G4A DNA in appropriate buffers (i.e., TE, Na^+, and K^+) were prepared. Appropriate amounts of stock solutions of either TMPyP2 or TMPyP4 were added sequentially to increase the molar ratio of porphyrin:DNA from 0:1 to 1:1, 2:1, and 5:1. Melting curves were obtained by monitoring the absorbance at 260 nm as the temperature was ramped from 20 to 95 °C at the rate of 0.5 °C/min. The temperatures corresponding to the maxima in the first derivative plots of melting curves were selected as the melting temperatures (T_m).

Hydroxyl-Radical Footprinting Studies. For each reaction, 10 μL of ^{32}P-labeled DNA 20 000 cpm (ca. 5 ng) was mixed with 10 μL of a 200 mM solution of either NaCl or KCl, and this mixture was boiled for 10 min and then cooled to room temperature. A 2.5 μL amount of a 10× hydroxyl reaction buffer [500 μM $Fe(NH_4)_2(SO_4)_2$, 1 mM Na_2-EDTA, 10 mM sodium ascobate] was added and reacted with 2.5 μL of 10% H_2O_2 for various times, as indicated in the caption to Figure 4. The reaction was stopped with 100 μL of stopping buffer (10 μL of 1 M thiourea, 10 μL of 3 M NaAc, 10 μL of 1 μg/μL tRNA, 10 μL of 1 μg/μL calf thymus DNA, 1 μL of 0.5 M EDTA, and 60 μL of H_2O). The DNA samples were then subjected to phenol extraction and ethanol precipitation. Finally, the DNA samples were boiled for 5 min and loaded onto a 16% polyacrylamide gel for electrophoresis.

Photocleavage Assay. G4A DNA was labeled with ^{32}P at the 5′-end and stored in 1× TE buffer at 2000 cpm/μL. For each photocleavage reaction, 10 μL of DNA (∼5 ng) was mixed with 10 μL of a 200 mM solution of KCl or NaCl and boiled for 10 min before cooling to room temperature. For the control samples, 10 μL of distilled water was added instead of NaCl or KCl. The reaction mixtures were transferred to a 96-well microtiter plate and mixed with 2 μL of 1 μM TMPyP4 or TMPyP2 aqueous solution. A glass filter was used to cover the microtiter plate, eliminating UV light under 300 nm and reducing evaporation. The samples were then exposed to a 24-watt fluorescent light for 0, 2, 5, 10, and 20 min, respectively. The reactions were stopped with 100 μL of calf thymus DNA (0.1 μg/μL). After phenol−chloroform extraction, the samples were subjected to strand breakage treatment and then ethanol precipitated.[14] Finally, the DNA samples were loaded onto a 16% denaturing polyacrylamide gel for electro-

(14) Han, F. X.; Hurley, L. H. *Biochemistry* **1996**, *35*, 7993−8001.

phoresis and visualized with a Phosphorimager (Molecular Dynamics Inc., model 445).

Results

The Design of the Intramolecular G4A Quadruplex DNA. DNA oligonucleotide G4A (sequence shown in Figure 2) was designed to form an intramolecular quadruplex DNA (Figure 2). It contains four repeats of the human telomere sequence 5′-GGGTTA that can fold independently into an intramolecular quadruplex DNA with a TTA diagonal loop.[15] We have used this intramolecular quadruplex structure as our key component for the G4A oligonucleotide design. At the flanking regions, a four-base-paired Watson−Crick duplex DNA was designed to form a stem, which further stabilizes the intramolecular quadruplex DNA. A linker region of three thymines was added at the 5′-end of the four GGGTTA repeats to connect the stem region with the intramolecular quadruplex structure. These three thymines were designed to create enough space between the quadruplex structure and the duplex stem to accommodate the TTA diagonal loop and to provide thymine−thymine hydrophobic interactions with it for additional stability. Another purpose for this stem region was to provide a duplex control DNA to compete with the quadruplex region for porphyrin binding. The protruding single-stranded end (5′-CATG) was designed for a DNA ligase assay, which was used to detect the formation of the duplex stem region. Formation of this stem region will limit the folding polarity of G4A DNA to an antiparallel orientation. Under different conditions, the G4A oligonucleotide may form other secondary structures, such as an intramolecular hairpin or foldover hairpin and a simple stem−loop (Figure 2).

Determination of the DNA Secondary Structure of the G4A Oligonucleotide under Different Buffer Conditions. Before the interactions of the porphyrin compounds with G4A DNA were studied, a series of experiments was initiated to determine the secondary structure of the G4A DNA in the three different buffers. A DNA ligase assay was first used to confirm the formation of a double-stranded stem region in the G4A DNA (Figure 2). If this double-stranded stem region exists, two molecules of the G4A DNA will form a duplex through the self-complementarity of their protruding single-stranded ends, and they can then be joined as a dimer by T4 DNA ligase. Therefore, the production of the G4A DNA dimers will implicate the formation of the duplex DNA stem. The denaturing gel electrophoresis experiments indicate that the same three ligation products of different mobility were observed under all three buffer conditions (Supporting Information). The ligation products were subjected to *Exo*III nuclease digestion, which is routinely used for the detection and removal of linear DNA. A quantitative phosphorimager measurement showed that the sum of the ligation products (both linear and circular dimers) accounted for 82% of the total DNA species produced under all three buffer conditions (data not shown). These results suggest that most of the G4A DNA molecules did not consist of random-coiled single-stranded DNA but rather a mixture of species that contains secondary structures with a Watson−Crick base-paired duplex stem. Finally, formation of this duplex stem indicates that the folding polarity of G4A is antiparallel under all three buffer conditions.

DMS Footprinting Suggests That G4A DNA Forms a Stable Intramolecular Quadruplex in the K^+ Buffer but Is a Mixture of Different Secondary Structures in the Na^+ Buffer. DMS footprinting was employed to further characterize the secondary structures of the four human telomere repeats in the G4A DNA. Since N7 of guanine is positioned in the major groove of a normal B-form DNA and is not involved in hydrogen bonding between GC base pairs, it can be methylated by DMS, leading to DNA strand cleavage upon piperidine treatment. The methylation reaction and subsequent strand cleavage can produce distinct bands corresponding to the reacting guanines when the DNA samples are subjected to gel electrophoresis. In quadruplex DNA involving guanine tetrads, four Hoogsteen base pairs are created (Figure 1). In the tetrad, N7 of each guanine is hydrogen-bonded to N2 of the adjacent guanine and is therefore protected from DMS methylation. In hairpin DNA formed by guanine−guanine Hoogsteen base pairing, only one N7 is involved in hydrogen bonding, and therefore only one of the guanines is protected from DMS. The DMS footprinting results of G4A DNA in TE, 100 mM Na^+, and 100 mM K^+ buffers are shown in Figure 3. In the control TE buffer (lanes 1−4), all guanines corresponding to the four GGGTTA repeats appear unprotected from DMS modification, suggesting no involvement of Hoogsteen hydrogen bonding. Therefore, guanines in this region did not form either guanine tetrads or guanine−guanine base pairs in TE buffer. We conclude that G4A forms a simple stem−loop structure (Figure 2) in the control TE buffer. In lanes 9−12 of Figure 3, in the 100 mM KCl buffer the complete DMS protection patterns in the GGGTTA repeat region indicate the formation of quadruplex DNA. Although both the hairpin-dimer/hairpin-foldover quadruplex and the intramolecular quadruplex (Figure 2) may generate this complete DMS protection pattern, the intramolecular quadruplex DNA is presumed to be favored as the dominant species in the K^+ buffer. As shown in lanes 5−8 of Figure 3, the GGGTTA repeats region was only slightly modified by DMS, with GGGTTA repeats III and IV reacting more strongly with DMS than repeats I and II. The DMS semi-protection patterns suggest the formation of a hairpin species and/or unstable quadruplex DNA; the latter may arise from the association of two hairpins. The different modification patterns within the four GGGTTA repeats region support this idea. The lower modifications by DMS in repeats I and II suggest that N7 of guanine in these regions is favored for hydrogen bonding with N2 of guanine in repeats IV and III. This hydrogen-bonding formation leaves N7 of guanine at repeats III and IV exposed to the solvent and therefore subject to DMS methylation. In view of the proposed antiparallel nature of the DNA in 100 mM Na^+ buffer (see later), we propose that the major species of G4A DNA are intramolecular hairpins, as shown in Figure 2. However, a G4A diagonal intramolecular quadruplex structure (Figure 2), which is less tightly bound in the Na^+ buffer, may also lead to the semi-protection pattern by DMS. Present experimental data cannot differentiate between these two possibilities. Under all three buffer conditions (i.e., TE, K^+, and Na^+ buffers), regions corresponding to the stem were modified by DMS to the same extent. These results strongly suggest that the GGGTTA repeats of G4A DNA form a simple loop in the TE buffer, a diagonal intramolecular quadruplex in the K^+ buffer, and a mixture of different possible secondary structures in the Na^+ buffer, including hairpin, hairpin-dimer quadruplex, unstable diagonal, and/or hairpin-foldover intramolecular quadruplexes. However, the double-stranded stem region remains the same under all buffer conditions.

CD Profiles Demonstrate That the Antiparallel Quadruplex Is the Dominant Species of G4A DNA Found under Na^+ and K^+ Buffer Conditions. CD was used to further characterize the solution conformation of the G4A DNA in

(15) Wang, Y.; Patel, D. J. *Structure* **1993**, *1*, 263−282.

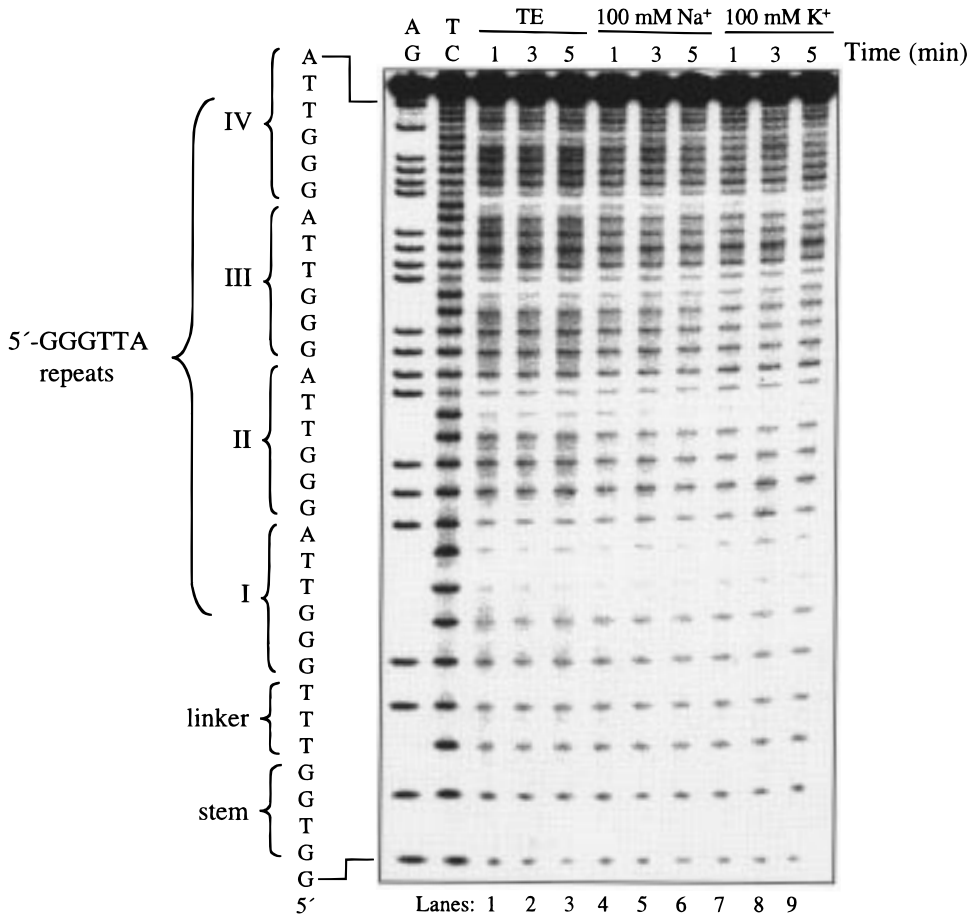

Figure 4. Hydroxyl-radical footprinting of G4A DNA in the TE, Na^+, and K^+ buffers. Lanes AG and TC are Maxam−Gilbert sequencing reactions. Lanes 1−3 are hydroxyl-radical footprinting reactions of G4A in the control TE buffer, corresponding to reaction times of 1, 3, and 5 min, respectively. Lanes 4−6 and 7−9 are the same reactions performed in the Na^+ and K^+ buffers, respectively. The partial sequence of G4A and its components is shown on the left side of the gel.

various buffers. Previous CD studies have established consistent assignments for parallel and antiparallel quadruplex DNA.[16,17] An antiparallel quadruplex is characterized by a positive CD peak near 290 nm and a negative CD peak near 260 nm. A parallel quadruplex is characterized by a positive CD peak near 260 nm and a negative CD peak near 240 nm.[18−21] The results in Supporting Information show the presence of strong positive peaks at 290 nm in the CD spectra of the G4A DNA in both Na^+ and K^+ buffers and a positive peak at 260 nm in the control TE buffer. Two shoulders are also shown at 260 nm in both Na^+ and K^+ buffers. Under all three buffer conditions, negative peaks are seen at 240 nm. The formation of strong positive peaks at 290 nm in both Na^+ and K^+ buffers confirmed that the predominant DNA species are antiparallel quadruplex DNA. The relatively stronger peak in the K^+ buffer agrees with the DMS footprinting results that G4A forms the more stable intramolecular quadruplex DNA in the K^+ buffer. In contrast, the relatively weaker peak at 290 nm is consistent with a hairpin-dimer or unstable intramolecular quadruplex DNA in the Na^+ buffer. The strong positive peak at 260 nm and the negative peak at 240 nm in the TE control buffer seem to implicate the formation of a parallel quadruplex DNA. This contrasts with the previous conclusion that G4A DNA forms an antiparallel simple stem−loop under the same conditions. To explain this inconsistency, we propose that the duplex DNA in the stem region can produce CD signals, which have a positive peak at 260 and a trough at 240 nm. This peak at 260 nm is partially offset in the Na^+ and K^+ buffers by the antiparallel quadruplex G4A DNA that creates a negative peak near the same wavelength. However, G4A DNA cannot offset this peak in the control TE buffer due to the absence of the antiparallel quadruplex DNA formation. This also explains the shoulders at 260 nm in both Na^+ and K^+ buffers, which represent the combined CD signals of both quadruplex and duplex DNA. On the basis of previous results from ligase assay and DMS footprinting experiments, considered together with these CD profiles, we propose that antiparallel quadruplex DNA structures are formed in both the Na^+ and K^+ buffers but not in the control TE buffer.

Hydroxyl-Radical Footprinting Shows No Significant Difference in the Cleavage Patterns of G4A in the TE, Na^+, and K^+ Buffers. Singlet oxygen intermediates such as the hydroxyl radical have been proposed to be responsible for the porphyrin-induced DNA photocleavage.[22] Hydroxyl-radical footprinting was used to assess how different modes of folding of G4A DNA in TE, Na^+, and K^+ buffers might affect the

(16) Lu, M.; Guo, Q.; Kallenbach, N. R. *Biochemistry* **1993**, *32*, 598−601.
(17) Balagurumoorthy, P.; Brahmachari, S. K.; Mohanty, D.; Bansal, M.; Sasisekharan, V. *Nucleic Acids Res.* **1992**, *20*, 4061−4067.
(18) Guo, Q.; Lu, M.; Kallenbach, N. R. *Biochemistry* **1993**, *32*, 3596−3603.
(19) Guo, Q.; Lu, M.; Marky, L. A.; Kallenbach, N. R. *Biochemistry* **1992**, *31*, 2451−2455.
(20) Hardin, C. C.; Watson, T.; Corregan, M.; Bailey, C. *Biochemistry* **1992**, *31*, 833−841.
(21) Gupta, G.; Garcia, A. E.; Guo, Q.; Lu, M.; Kallenbach, N. R. *Biochemistry* **1993**, *32*, 7098−7103.
(22) Nussbaum, J. M.; Newport, M. E.; Mackie, M.; Leontis, N. B. *Photochem. Photobiol.* **1994**, *59*, 515−528.

accessibility of each nucleotide to hydroxyl free radical. Figure 4 is a time-dependent hydroxyl-radical footprinting experiment performed on the G4A DNA. In the stem region (the bottom portions of lanes 1−9), the cleavage patterns and intensities of the four nucleotides are almost identical under all three buffer conditions. This result is consistent with the previous observation that the stem region forms the same secondary structure in the TE, Na^+, and K^+ buffers. In the linker region (middle portions of lanes 1−9), the three thymines were cleaved weakly. No significant difference in cleavage patterns was observed under the TE, Na^+, and K^+ buffer conditions. In the four telomere repeats region (the top portions of lanes 1−9), G4A was cleaved slightly more strongly in the TE buffer than in either the Na^+ or K^+ buffer. Under each buffer condition, the guanine nucleotides within each telomere repeat were not cleaved evenly; however, the differences in cleavage intensities at these guanines were not distinct enough to establish a clear selectivity. Overall, these hydroxyl-radical footprinting results suggest that the different secondary structures of G4A formed under different buffer conditions do not affect the accessibility of the G4A DNA to hydroxyl-radical cleavage. Furthermore, these results imply that the selective photocleavage of G4A DNA by the porphyrin compounds TMPyP4 and TMPyP2 (see later) was not achieved at the step of DNA cleavage induced by singlet oxygen intermediates. More likely, it was predetermined by where these DNA cleaving species were generated, which was decided at the structure recognition step between the porphyrins and G4A DNA. Therefore, the photocleavage selectivity of porphyrin compounds reflects the binding preference of porphyrins to G4A DNA.

UV Studies Show That TMPyP4 and TMPyP2 Increase the Melting Temperatures of Quadruplex DNA by about the Same Amount. The thermal melting profiles of G4A DNA alone in both Na^+ and K^+ buffers are shown in Figure 5A. G4A DNA has a narrower thermal transition range and a higher melting temperature in the K^+ buffer than in the Na^+ buffer. This observation is consistent with the results from DMS footprinting that G4A DNA forms a more stable intramolecular quadruplex DNA in the K^+ buffer but a less stable hairpin-dimer and/or unstable intramolecular quadruplex DNA in the Na^+ buffer. Figure 5B shows the thermal melting profiles of TMPyP4/G4A and TMPyP2/G4A complexes in both Na^+ and K^+ buffers as a function of the mixing ratios of porphyrin to DNA. In the K^+ buffer, the melting temperature increases from below 50 °C for G4A DNA alone to over 57 °C as the molar ratio of porphyrin to DNA increases from 0 to 5 for both TMPyP2 and TMPyP4. The same increment of temperature increase is also observed in the Na^+ buffer, although the initial melting temperatures of G4A in the absence of TMPyP2 and TMPyP4 are lower. The TMPyP4-induced melting temperature increase (ΔT_m) in the Na^+ buffer appears to be slightly larger than that induced by TMPyP2. Overall, however, these concentration-dependent thermal melting results show that both TMPyP2 and TMPyP4 stabilize quadruplex DNA to about the same extent (i.e., about 8−9 °C at the porphyrin to DNA ratio of 5:1) in both Na^+ and K^+ buffers.

Photocleavage of G4A DNA by TMPyP4 in the K^+ Buffer Demonstrates That TMPyP4 Binds to Quadruplex DNA by External Stacking to the G-Tetrads. The intrinsic DNA photocleavage ability of the porphyrins was used to detect the precise positions at which TMPyP4 and TMPyP2 bind to the G4A DNA secondary structure. In the porphyrin-mediated photocleavage reaction with DNA, either the deoxyribose or the base is damaged, although the precise reaction mechanisms

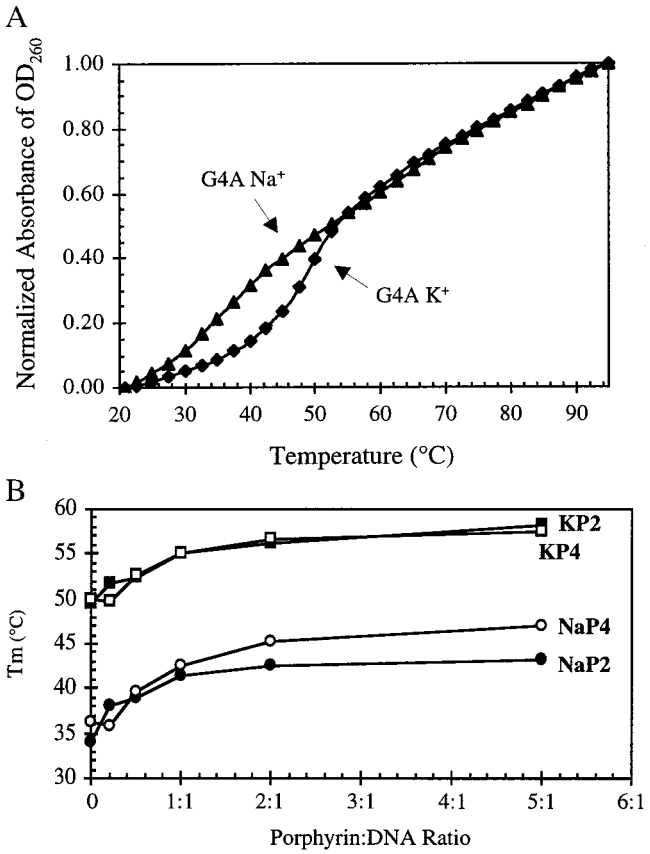

Figure 5. (A) The UV melting profiles of G4A DNA in the Na^+ (▲) and the K^+ (◆) buffers. (B) The effects of mixing ratio on the melting temperatures of G4A/porphyrin complexes. Series NaP2 (●) represents the G4A/TMPyP2 complexes in the Na^+ buffer. Series KP2 (■) represents the G4A/TMPyP2 complexes in the K^+ buffer. Series NaP4 (○) represents the G4A/TMPyP4 complexes in the Na^+ buffer. Series KP4 (□) represents the G4A/TMPyP4 complexes in the K^+ buffer.

are still unclear.[23,24] In either case, DNA strand breakage can be induced when the porphyrin-damaged DNA is subjected to piperidine treatment. In the control TE buffer, the time-dependent photocleavage reactions in Figure 6A (lanes 1−5) show that TMPyP4 reacts more strongly with the 5′-GGGTTA repeat region than with the stem region. The weaker cleavage at the stem region in the same reaction is consistent with the previous observations that porphyrin prefers to bind to single-stranded rather than double-stranded DNA.[24] Moreover, within each repeat, all three guanines are cleaved almost equally by TMPyP4; however, under K^+ buffer conditions (lanes 6−9), distinct selective patterns are observed. TMPyP4 specifically cleaves the guanines corresponding to G1, G6, G7, and G12 in 100 mM KCl. From the DMS footprinting experiment, we propose that G4A DNA primarily forms an intramolecular quadruplex DNA with a diagonal loop (see Figure 6A). This folding pattern places G1, G6, G7, and G12 within the same guanine tetrad. Selective photocleavage at these guanines strongly suggests that porphyrin binds to G4A DNA by stacking *externally* to the G1-G6-G7-G12 tetrad. Intercalation of TMPyP4 *between* guanine tetrads is less likely, since G2, G5, G8, and G11 were not cleaved at the early time points. External stacking of TMPyP4 to a foldover hairpin quadruplex DNA (Figure 6A) formed by G4A DNA would also produce the same photo-

(23) Pratviel, G.; Pitie, M.; Bernadou, J.; Meunier, B. *Nucleic Acids Res.* **1991**, *19*, 6283−6288.
(24) Saito, T.; Kitamura, M.; Tanaka, M.; Morimoto, M.; Segawa, H.; Shimidzu, T. *Nucleic Acids Symp. Ser.* **1993**, *29*, 127−128.

cleavage pattern; however, this foldover hairpin quadruplex formation in K^+ is less likely and if present is only likely to account for a small percentage of the total G4A species formed in K^+ (see later).

Photocleavage of G4A DNA by TMPyP4 in the Na^+ Buffer Demonstrates That TMPyP4 Adopts an External Stacking Mode to Interact with the Hairpin-Dimer and/or the Unstable Intramolecular Quadruplex DNA. The photocleavage of G4A DNA by TMPyP4 in the Na^+ buffer is shown in Figure 6B. TMPyP4 selectively cleaves at G1, G4, G6, G7, G9, and G12. On the basis of the DMS footprinting experiment, we propose that G4A DNA forms a hairpin-dimer quadruplex and perhaps an unstable intramolecular quadruplex DNA. The hairpin-dimer model is used to explain the TMPyP4 photocleavage pattern since explanations based upon the unstable intramolecular quadruplex model are the same as those for photocleavage patterns in the K^+ buffer, as previously described. Photocleavage at G1, G6, G7, and G12 can be rationalized by a model involving external stacking of TMPyP4 to a six-layered hairpin-dimer quadruplex of G4A, as indicated in the top diagram of Figure 6B. Photocleavage at the G4 and G9 positions can only be explained by the stacking of TMPyP4 to a three-layered hairpin-dimer quadruplex DNA (bottom diagram in Figure 6B). Under both Na^+ and K^+ buffer conditions, TMPyP4 cleaves the quadruplex region much more strongly than the Watson−Crick duplex stem region, suggesting that quadruplex DNA is favored over duplex DNA for TMPyP4 binding.

Photocleavage of G4A DNA by TMPyP2 in the K^+ Buffer Demonstrates That TMPyP2 Interacts with Quadruplex DNA by Binding from outside the TTA Loop. The time-dependent photocleavage of G4A DNA by TMPyP2 in the TE and K^+ buffers is shown in Figure 7A. TMPyP2 produces indiscriminate cleavage at all of the guanines in the quadruplex region in the TE control buffer but much more selective cleavage in the K^+ buffer. In the K^+ buffer, the major photocleavage sites are six specific thymines. In addition, there is weaker cleavage at G1, G6, G7, and G12, similar to the pattern that was observed in the K^+ buffer for the TMPyP4 photocleavage. On the basis of the previously described DMS footprinting results, we propose that G4A DNA folds into a diagonal intramolecular quadruplex in the K^+ buffer. To explain the strong selective cleavage at the thymines shown in Figure 7A, we also propose that TMPyP2 binds to G4A quadruplex DNA outside the TTA diagonal loop (bottom diagram in Figure 7A). This binding mode positions the TMPyP2 molecule in the vicinity of the thymine linker, the TTA diagonal loop, and the TTA of the last GGGTTA repeat. To explain the weak photocleavage of G4A DNA by TMPyP2 at G1, G6, G7, and G12 in the K^+ buffer, we suggest that a small amount of TMPyP2 can stack to the guanine tetrad and cause photocleavage in a manner similar to TMPyP4 (the top diagram in Figure 7A). Since the six thymines are cleaved much more strongly than the guanines, these results indicate that TMPyP2 interacts with the G4A DNA primarily by binding from outside the TTA diagonal loop.

Photocleavage of G4A DNA by TMPyP2 in the Na^+ Buffer Demonstrates That TMPyP2 Adopts the Outside Binding Mode to Interact with the Hairpin-Dimer and/or the Unstable Intramolecular Quadruplex DNA. The photocleavage patterns produced by TMPyP2 in the Na^+ buffer are shown in Figure 7B. Lanes 1−5 are time-dependent photocleavage assays performed in the control TE buffer as previously described. The results in lanes 6−10 show that TMPyP2 photocleaves G4A DNA weakly at the G1, G4, G6, G7, G9, and G12 positions but strongly at the same six thymines, as seen in the TMPyP2 photocleavage reaction in the K^+ buffer. The hairpin-dimer model rather than the unstable intramolecular G4A DNA model (Figure 7A) was used to explain the TMPyP2 photocleavage patterns for the same reason as addressed in the previous section. These photocleavage patterns can be rationalized by interactions of TMPyP2 with the six-layered and three-layered hairpin-dimer quadruplex DNA that are proposed to be formed in the Na^+ buffer. Direct external stacking of TMPyP2 to the G-tetrad in the six-layered and three-layered hairpin-dimer quadruplex DNA results in the less intense photocleavage at G1, G4, G6, G7, G9, and G12 (top diagram in Figure 7B). However, binding of TMPyP2 from outside the TTA loop of the same G4A secondary structures will produce the observed stronger photocleavage at the six thymines (bottom diagram in Figure 7B). Because the six thymines are cleaved more strongly than the guanines, these results indicate that TMPyP2 interacts with the hairpin-dimer and/or unstable intramolecular quadruplex DNA primarily by binding from outside the middle TTA loop.

Discussion

Using a ligase assay, DMS footprinting, and a CD spectroscopic study, we have characterized the secondary structures of G4A DNA in different buffers. These experiments led us to conclude that G4A DNA forms an intramolecular quadruplex in the K^+ buffer and a mixture of hairpin, hairpin-dimer quadruplex, and perhaps an unstable intramolecular quadruplex in the Na^+ buffer. Analysis of the data from UV melting temperature studies shows that both TMPyP2 and TMPyP4 stabilize the antiparallel quadruplex DNA structure to about the same extent. The results from photocleavage assays in the K^+ buffer demonstrate that while TMPyP4 interacts with intramolecular quadruplex DNA by external stacking between the outer layer of the guanine tetrad and the TTA diagonal loop, TMPyP2 interacts with the same quadruplex DNA by binding outside the same TTA diagonal loop. In the Na^+ buffer, TMPyP4 also binds to the hairpin-dimer quadruplex DNA and perhaps to the unstable intramolecular quadruplex DNA by external stacking to the outside layer of the guanine tetrad, while TMPyP2 binds to the same quadruplex DNA from outside the TTA loop of the second GGGTTA repeat.

TMPyP4 Interacts with Quadruplex DNA by External Stacking to the G-Tetrads instead of Intercalating between Adjacent G-Tetrads. The cationic porphyrin TMPyP4 has the appropriate physical-chemical properties for intercalating between guanine tetrads, including a similar molecular size, a flat porphine chromophore, free rotatable pyridyl substituents, and positive charges. However, such intercalation would have to disrupt the very stable quadruplex DNA structure, which is energetically extremely unfavorable. The more favored binding is apparently via stacking at the end of the guanine tetrad while leaving the quadruplex DNA network intact. In a time-dependent photocleavage assay, we demonstrated that TMPyP4 selectively cleaves guanines at the external G1-G6-G7-G12 tetrad of the G4A intramolecular quadruplex DNA. This result seems to be in conflict with the favored intercalation models recently proposed in similar studies using parallel quadruplex DNA.[25] If TMPyP4 intercalates between the guanine tetrads in the G4A quadruplex DNA, we would expect strong photocleavages at the G2-G5-G8-G11 tetrad. In a molecular modeling study carried out by docking the TMPyP4 molecule into the NMR structure of $d(AG_3[T_2AG_3]_3)$ intramolecular quadruplex DNA,[15] it was

(25) (a) Anatha, N. V.; Mahrukh, A.; Sheardy, R. D. *Biochemistry* **1998**, *37*, 2709−2714. (b) Haq, I.; Trent, J. O.; Chowdhry, B. Z.; Jenkins, T. C. *J. Am. Chem. Soc.* **1999**, *121*, 1768−1779.

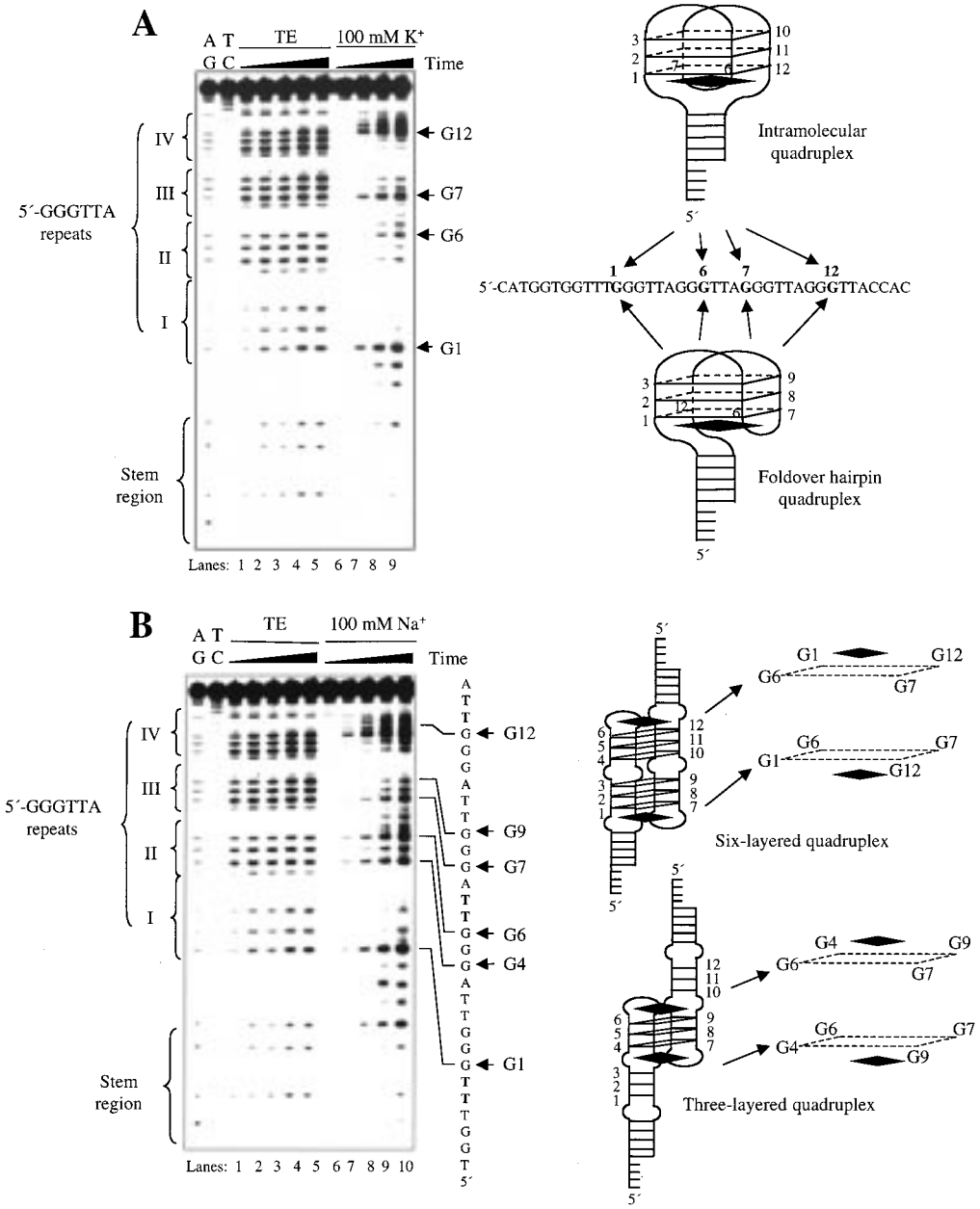

Figure 6. (A) Time-dependent photocleavage assay of G4A DNA by TMPyP4 in the control TE buffer and the K^+ buffer. Lanes AG and TC are the Maxam−Gilbert sequencing reactions. Lanes 1−5 are photocleavage assay of G4A by TMPyP4 performed in the control TE buffer for 0, 2, 5, 10, and 20 min, respectively. Lanes 6−9 are the same reactions performed in the K^+ buffer. The two diagrams on the right represent the two hypothetical secondary folding structures (the intramolecular and foldover hairpin quadruplexes) of G4A DNA formed in the K^+ buffer. TMPyP4 molecules (represented by the black squares) interact with these two secondary structures by external stacking. The sequence information on each side of the gel and between the diagrams on the right corresponds to G4A in Figure 2. (B) Time-dependent photocleavage assay of G4A DNA by TMPyP4 in the control TE buffer and the Na^+ buffer. Lanes AG and TC are the Maxam−Gilbert sequencing reactions. Lanes 1−5 are photocleavage assays of G4A by TMPyP4 performed in the control TE buffer for 0, 2, 5, 10, and 20 min, respectively. Lanes 6−10 are the same reactions performed in the Na^+ buffer. The two diagrams on the right represent the two hypothetical secondary folding structures (the six-layered and three-layered hairpin dimer quadruplexes) of G4A DNA formed in the Na^+ buffer. The TMPyP4 molecules (represented by the black squares) interact with these two secondary structures by external stacking to the guanine tetrads. The sequence information for G4A is provided on both sides of the gel.

found that external stacking of TMPyP4 with the G3-G4-G9-G10 tetrad was extremely unfavorable compared with the G1-G6-G7-G12 tetrad (Langley and Hurley, unpublished results). The higher energy cost for the former stacking comes from the steric repulsion within porphine and between the porphine and the tetrad intercalation cleft. The dihedral angles between the porphine core and the pyridyl substitution groups are ∼60° when TMPyP4 is stacked outside and against the G1-G6-G7-G12 tetrad and ∼44° when intercalated between tetrads (assuming a rise of 6.4 Å between tetrads). For TMPyP4, the energy cost for the concerted rotation of all four pyridyl groups from the minima of ∼80 to ∼60° is ∼2.8 kcal/mol. The continued rotation to ∼40° costs an additional ∼13.6 kcal/mol. For TMPyP2, the energy cost for the concerted rotation of all four pyridyl groups from the minima of ∼80 to ∼60° is ∼6.2 kcal/mol. The continued rotation to ∼40° costs an additional ∼25.0 kcal/mol. Taking these modeling predictions with the results from the photocleavage experiments, we strongly favor a model in which TMPyP4 interacts with the G4A intramolecular

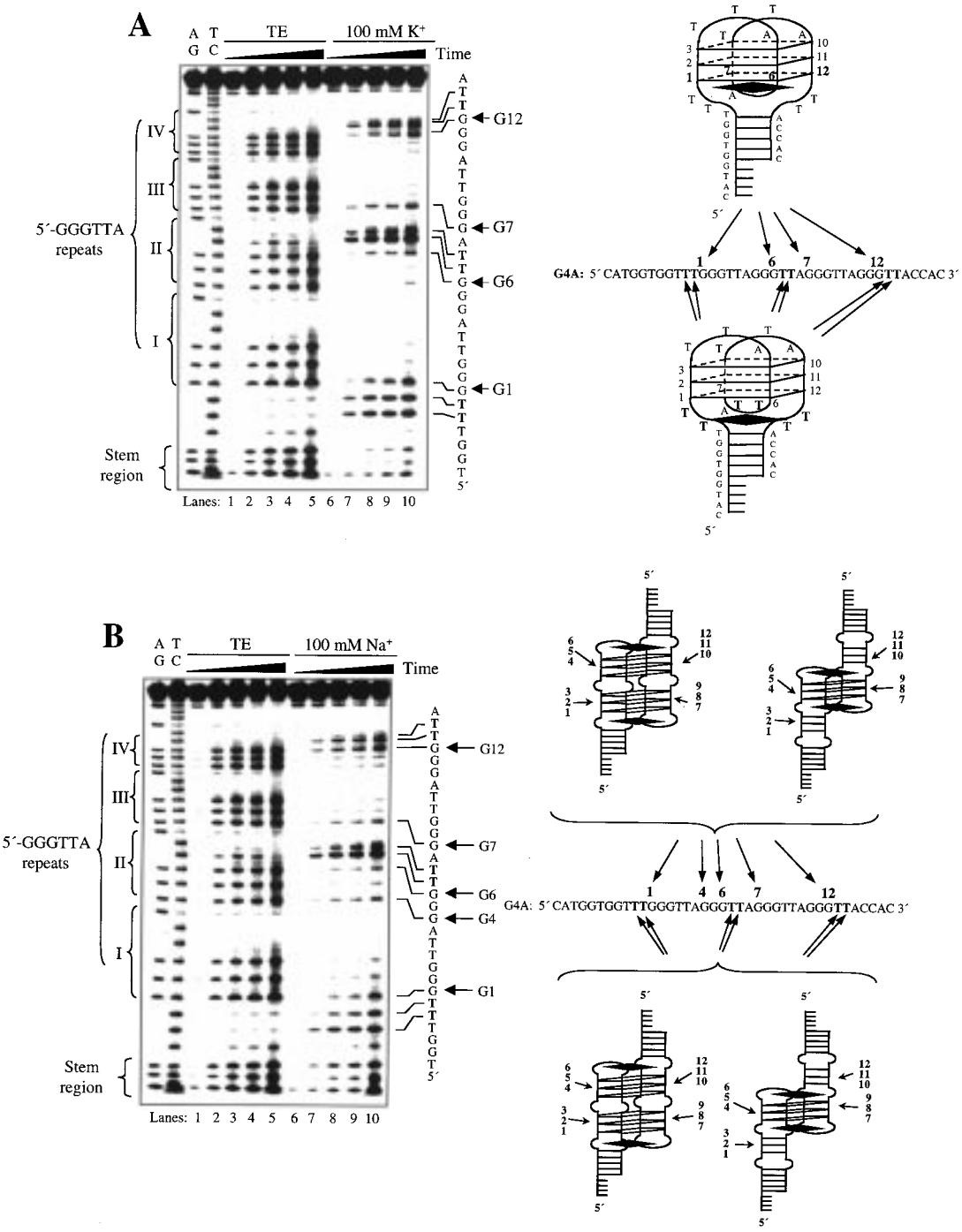

Figure 7. (A) Time-dependent photocleavage assay of G4A DNA by TMPyP2 in the control TE buffer and the K^+ buffer. Lanes AG and TC are the Maxam−Gilbert sequencing reactions. Lanes 1−5 are photocleavage assays of G4A by TMPyP2 performed in the control TE buffer for 0, 2, 5, 10, and 20 min, respectively. Lanes 6−10 are the same reactions performed in the K^+ buffer. The top diagram on the right shows that a small amount of TMPyP2 (represented by the black square) stacks to the G1-G6-G7-G12 tetrad to generate weak photocleavage at these sites. The bottom diagram on the right shows that the majority of TMPyP2 binds to the intramolecular quadruplex DNA from outside the TTA diagonal loop to create photocleavage at the six selective thymines (boldface bases in the G4A sequence on the right side of the gel). (B) Time-dependent photocleavage assay of G4A DNA by TMPyP2 in the control TE buffer and the Na^+ buffer. Lanes 1−5 are photocleavage assays of G4A by TMPyP2 performed in the control TE buffer for 0, 2, 5, 10, and 20 min, respectively. Lanes 6−10 are the same reactions performed in the Na^+ buffer. The top two diagrams on the right show the two molecules of TMPyP2 (represented by black squares) stacked externally to the six-layered and three-layered hairpin dimer quadruplexes to generate photocleavage at G1, G4, G6, G7, and G12. The bottom two diagrams on the right show that TMPyP2 binds to the six-layered and three-layered hairpin dimer quadruplexes from outside the TTA middle loop to produce photocleavage at the six selective thymines (boldface bases in the G4A sequence). Sequence information on both sides of the gel and between the diagrams on the right refers to G4A in Figure 2.

quadruplex DNA by a one-side external stacking with the G1-G6-G7-G12 guanine tetrad and within the diagonal TTA loop.

Structural Basis for the Differential Binding Modes of TMPyP2 and TMPyP4 to Quadruplex DNA. The cationic porphyrins TMPyP2 and TMPyP4 each have a porphine chromophore and four pyridyl rings substituted at the meso positions. They are both similar in size to a guanine tetrad (Figure 1) and can potentially intercalate or stack with the

guanine tetrads. However, the photocleavage results show that they each interact quite differently with G4A DNA. TMPyP4 binds to quadruplex DNA primarily by stacking with the outer layer of the guanine tetrad. In contrast, the main mode of TMPyP2 binding to G4A DNA is external to the TTA loops (the diagonal loop for an intramolecular quadruplex and the middle TTA loop for the hairpin-dimer quadruplex). We rationalize that the different quadruplex DNA binding modes of TMPyP4 and TMPyP2 are due to the conformational rotational difference of the pyridyl-rings in each ligand. In TMPyP4, the four meso-pyridyl rings are amenable to rotation and can easily become coplanar with the porphine chromophore. Therefore, TMPyP4 molecules can easily become flat to thread externally to the bottom layer of the guanine tetrad in the G4A DNA quadruplex. However, in TMPyP2, due to the steric repulsion between the 2-methyl groups in the pyridyl rings and the β-hydrogens in the porphine core, there is a high-energy barrier for the pyridyl rings to become coplanar with the porphine. At physiological temperatures, the pyridyl rings are locked primarily into a conformation that is perpendicular to the porphine core. Furthermore, the methyl groups on the pyridine rings lie partially over the face of the porphyrin ring, posing a $\pi-\pi$ stacking interaction and also increasing the *thickness* of TMPyP2 relative to TMPyP4. Due to this constraint, TMPyP2 cannot easily stack externally to the bottom guanine tetrad layer in the G4A quadruplex DNA and therefore fits more easily into the larger niche created by the diagonal loop and the thymine loops at the quadruplex−duplex junction. This explains the major TMPyP2 photocleavage sites at the six specific thymines. However, a small contributor to the TMPyP2 mixture of rotamers must be that which has all four *N*-methyl groups on the same face of the porphyrin, uniquely leaving the opposite face available for stacking. This would account for the weak photocleavage at the G1-G6-G7-G12 tetrad. This presumably accounts for the residual telomerase inhibition of TMPyP2.

Biological Implications of the Differential Interactions of TMPyP4 and TMPyP2 with Quadruplex DNA. It is interesting that both compounds stabilize quadruplex to about the same extent. Although stabilization of quadruplex DNA may be important for telomerase inhibition, it is how the stabilization is produced that appears to be more important. Since the different binding modes of TMPyP4 and TMPyP2 to quadruplex DNA are correlated to their telomerase inhibition potency, our results indicate that external stacking to the guanine tetrad is more efficient in producing telomerase inhibition than binding from outside.[26] In that sense, ortho-substitution groups that cannot become coplanar with the porphine platform are disfavored for telomerase inhibitor design. In addition, biological effects such as chromosomal aberrations and inhibitions of cell growth are associated only with TMPyP4 and are therefore correlated only with external stacking to the guanine tetrads[27] rather than stabilization of quadruplex structure.

Acknowledgment. We thank Violetta Chemeris and Brian Cathers for technical assistance and Oleg Fedoroff, Robb Gardner, and Haiyong Han for helpful discussions. We are very grateful to David Langley of Bristol-Myers Squibb, who provided the molecular modeling insight. We also thank Miguel Salazar and Robb Gardner for critical reading of the manuscript and David Bishop for proofreading, editing, and preparing the final version of the manuscript.

JA984153M

(26) The G4A sequence, d[CATG**GTGG**TTT(GGGTTA)$_4$ **CCAC**], used in this study contains an artificial double-stranded stem (bold). This stem sequence is not present in the human telomeric sequence, and therefore the double stranded stem is presumably missing in the human telomeric structure. The addition of the double-stranded stem has been useful in defining a high affinity binding site for TMPyP2. It is doubtful, however, that this alternative site has any biological relevance.

(27) Izbicka, E.; Wheelhouse, R. T.; Raymond, E.; Davidson, K. L.; Lawrence, R. A.; Sun, D.; Windle, B. E.; Hurley, L. H.; von Hoff, D. D. *Cancer Res.* **1999**, *59*, 639−644.